Available online at www.sciencedirect.com
SCIENCE DIRECT®
Journal of Solid State Chemistry 177 (2004) 2237–2241
JOURNAL OF SOLID STATE CHEMISTRY
http://elsevier.com/locate/jssc

Fabrication and luminescent properties of rare earths-doped $Gd_2(WO_4)_3$ thin film phosphors by Pechini sol–gel process

M.L. Pang, J. Lin,* and M. Yu

Key Laboratory of Rare Earth Chemistry and Physics, Changchun Institute of Applied Chemistry, Chinese Academy of Sciences, Changchun 130022, China

Received 29 October 2003; received in revised form 12 February 2004; accepted 18 February 2004

Abstract

Rare earth ions (Eu^{3+} and Dy^{3+})-doped $Gd_2(WO_4)_3$ phosphor films were prepared by a Pechini sol–gel process. X-ray diffraction (XRD), Fourier transform infrared spectroscopy (FT-IR), atomic force microscopy (AFM) and photoluminescence (PL) spectra as well as lifetimes were used to characterize the resulting powders and films. The results of XRD indicate that the films begin to crystallize at 600°C and the crystallinity increases with the elevation of annealing temperatures. The film is uniform and crack-free, mainly consists of closely packed fine particles with an average grain size of 80 nm. Owing to an energy transfer from WO_4^{2-} groups, the rare earth ions show their characteristic emissions in crystalline $Gd_2(WO_4)_3$ phosphor films, i.e., $^5D_J-^7F_{J'}$ ($J=0$, 1, 2, 3; $J'=0$, 1, 2, 3, 4, not in all cases) transitions for Eu^{3+} and $^4F_{9/2}-^6H_J$ ($J=13/2$, 15/2) transitions for Dy^{3+}, with the hypersensitive transitions $^5D_0-^7F_2$ (Eu^{3+}) and $^4F_{9/2}-^6H_{13/2}$ (Dy^{3+}) being the most prominent groups, respectively. Both the lifetimes and PL intensity of the Eu^{3+} ($^5D_0$) and Dy^{3+} ($^4F_{9/2}$) increase with increasing the annealing temperature from 500°C to 800°C, and the optimum doping concentrations for Eu^{3+} and Dy^{3+} are determined to be 30 and 6 at% of Gd^{3+} in $Gd_2(WO_4)_3$ film host lattices, respectively.
© 2004 Elsevier Inc. All rights reserved.

Keywords: Europium; Dysprosium; $Gd_2(WO_4)_3$; Thin film phosphors; Pechini sol–gel process

1. Introduction

It is well known that rare earth elements can form a series of isomorphous tungstates with general formula $RE_2(WO_4)_3$ (RE = rare earth elements), and some of these compounds show interesting fluorescence properties [1]. Nassau et al. [2] and Borchardt [3] have prepared this series of compounds and studied their structures, respectively. Since then, few reports about preparation of $Gd_2(WO_4)_3$ can be found. Until recently, Kodaira et al. [4] reported the preparation of $RE_2(WO_4)_3$:Eu (RE = La, Gd) powders using the Pechini method.

So far luminescent films have played an important role in high-resolution devices such as cathode-ray tubes (CRTs), electroluminescent devices (ELDs), plasma display panels (PDPs) and field emission displays (FEDs) [5]. Displays with thin film phosphors have higher contrast and resolution, superior thermal conductivity as well as a high degree of uniformity and better adhesion [6]. Nowadays, solid state reaction and Czochralski method are still the most often used methods to prepare $Gd_2(WO_4)_3$ phosphors and crystals [1–3]. Generally, these techniques always need high temperature or a long time heating. Therefore, a simple and economical method for making high quality luminescent films is desirable. Recently, spray pyrolysis has been developed to deposit thin film phosphors because it takes advantages in tailoring materials composition and large-scale deposition [7–9]. Another important techniques for the synthesis of various functional coating films is the solution-based sol–gel method, because it possesses a number of advantages over conventional film formation techniques, such as low temperature processing, easy coating of large surfaces, and possible formation of porous films and homogeneous multicomponent oxide films [10]. In fact, some efforts have been made to develop various kinds of luminescent films via sol–gel method in the past decade. Representative examples are $Y_3Al_5O_{12}$:Tb [5] and

*Corresponding author. Fax: +86-431-5698041.
E-mail address: jlin@ns.ciac.jl.cn (J. Lin).

0022-4596/$ - see front matter © 2004 Elsevier Inc. All rights reserved.
doi:10.1016/j.jssc.2004.02.031

Y_2SiO_5:Tb [6] films for cathodoluminescence, $Y_3Al_5O_{12}$:Eu [11] films for field emission displays, Y_2O_3:Eu [12] and Zn_2SiO_4:Mn [13] films for photoluminescence. In most of the above cases, the sol–gel precursors used are metal alkoxides and/or organometallic compounds, which suffer from high cost, toxicity and difficulty in controlling the experimental processes. An alternative approach to form thin film is the Pechini-type sol–gel process, which mainly employs the inorganic salts as precursors, citric acid as chelate ligand and polyethylene glycol (PEG) as cross-linking agent [14].

In view of the high cost and toxicity of the alkoxide precursors used in the conventional sol–gel process, we report a Pechini sol–gel synthesis of the rare earth ions (Eu^{3+} and Dy^{3+})-doped $Gd_2(WO_4)_3$ thin film phosphors and their photoluminescence properties in this paper.

2. Experimental

The thin film phosphor samples of $Gd_{2(1-x)}RE_{2x}(WO_4)_3$ ($0 \leqslant x \leqslant 0.5$; RE = Eu and Dy) were prepared by a Pechini sol–gel and dip-coating method [15]. Stoichiometric amounts of Gd_2O_3 (99.99%), Eu_2O_3 (99.99%) and Dy_2O_3 (99.99%) were dissolved in dilute HNO_3 (A.R., analytical reagent) under vigorous stirring, and the pH value of the solution was kept between two and three. Then stoichiometric amount of ammonium tungstate $(NH_4)_{10}W_{12}O_{41} \cdot 5H_2O$ (Fluka, A.R.) and a suitable amount of water–ethanol solution containing citric acid (A.R.) as chelating agent for the metal ions were added to the solution. The molar ratio of metal ions to citric acid was 1:2. Certain amount of polyethylene glycol (PEG, molecular weight = 10000, A.R.) was added as cross-linking agent. Highly transparent sols were obtained after stirring for a few hours, which were subsequently used for film deposition.

Silica glasses were used as the substrates. The thoroughly cleaned silica glass substrates were dipped into the sols and withdrawn at a speed of $0.5\,cm\,s^{-1}$. The as-formed transparent films were dried at 120°C immediately to drive off the remaining solvent. Then the films were annealed to high temperatures (400–800°C) with a heating rate of $60°C\,h^{-1}$ and held at each temperature for 2 h, respectively.

The X-ray powder diffraction (XRD) of the film samples was examined on a Rigaku-Dmax 2500 diffractometer using Cu$K\alpha$ radiation ($\lambda = 0.154056\,nm$). FT-IR spectra were measured with Perking-Elmer 580B infrared spectrophotometer with the KBr pellet technique. The morphology of the films was measured on an atomic force microscope (AFM, Seiko) with a tapping mode. The thickness of the films was obtained on an AUEL-III automatic laser ellipsometer. The excitation and emission spectra were obtained on a F-4500 spectrofluorimeter equipped with a 150 W xenon lamp as the excitation source. Luminescence lifetimes were measured with a SPEX 1934D phosphorimeter using a 7 W pulse xenon lamp as the excitation source with the pulse width of 3 μs. All the measurements were performed at room temperature.

3. Results and discussion

3.1. Formation process and morphology of the phosphor films

3.1.1. XRD

Fig. 1 shows the XRD profiles of the $Gd_{1.9}Eu_{0.1}(WO_4)_3$ films annealed from 500°C to 800°C. For the films annealed at 500°C, no diffraction peak is observed except for a broad band at $2\theta \approx 24°$, which is ascribed to silica glass substrate. This indicates that the film remains amorphous at/or below this annealing temperature. For the sample fired at 600°C, several strong diffraction peaks at $2\theta \approx 18.4°$, 27.8°, 29.1°, 31.0°, 34.1° and 46.9° are present in the XRD pattern, which are assigned to (111), (221), (023), (040), (204) and (242) reflections of monoclinic $Gd_2(WO_4)_3$ (JCPDS Card #23-1076) respectively, suggesting the starting of crystallization at this stage. Further increasing the annealing temperature to 800°C leads these peaks to become sharper and stronger due to the increase of crystallinity. All the diffraction peaks are in complete agreement with those of the JCPDS Card #23-1076 for $Gd_2(WO_4)_3$.

3.1.2. FT-IR

The FT-IR spectra of the $Gd_{1.9}Eu_{0.1}(WO_4)_3$ gel powders annealed from 100°C to 800°C are shown in

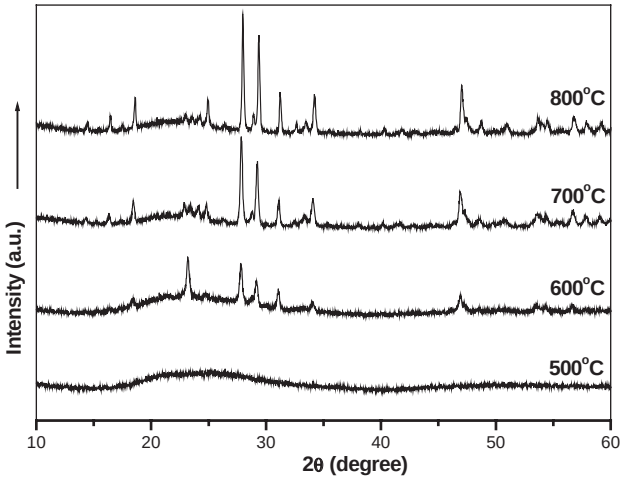

Fig. 1. X-ray diffraction patterns for $Gd_{1.9}Eu_{0.1}(WO_4)_3$ films annealed at different temperatures.

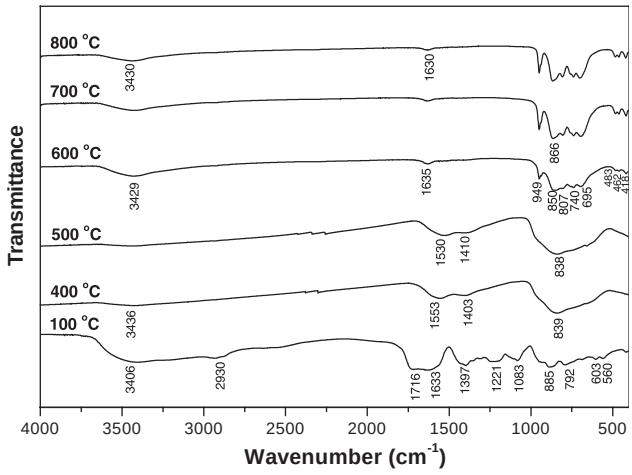

Fig. 2. FT-IR spectra of $Gd_{1.9}Eu_{0.1}(WO_4)_3$ precursor powders annealed at different temperatures.

Fig. 2. For the sample dried at 100°C, the FT-IR spectrum shows several broad absorption bands of −OH group (3407 cm^{-1}), $-CH_2$ group (2932 cm^{-1}), NO_3^- group (1720 and 1628 cm^{-1}), carbonates COO^- group (1399 cm^{-1}) and $W_{12}O_{41}^{10-}$ group (1083, 887, 791, 603 and 559 cm^{-1}), all of which arise from the starting materials such as citric acid, PEG, $Eu(NO_3)_3$, $Gd(NO_3)_3$ and $(NH_4)_{10}W_{12}O_{41}\cdot 5H_2O$ etc., as observed previously [15–17]. The absorption intensity of these bands decreased with increasing the sintering temperature due to the pyrolysis of the organic species. For the sample annealed between 400°C and 500°C, a strong broad absorption band at 839 cm^{-1} as well as several weak ones at 3436, 1553 and 1403 cm^{-1} can be observed in the FT-IR spectrum. The former may be due to the vibration of WO_4 unit in the starting material $(NH_4)_{10}W_{12}O_{41}\cdot 5H_2O$, and the latter should be assigned to the organic impurities. This indicates that the organic species have not decomposed completely and $Gd_2(WO_4)_3$ has not formed at this stage. After heating at 600°C, several split absorption peaks at 949, 850, 807, 740, 695, 483, 462 and 419 cm^{-1} have appeared, which belong to the $Gd_2(WO_4)_3$ phase [4]. This suggests that crystalline $Gd_2(WO_4)_3$ has formed at this temperature (600°C), agreeing basically with the results of XRD. After further heat treatment from 700°C to 800°C, the W–O bond turns stronger due to the improvement of the crystallinity with increasing the annealing temperature. At 800°C, there are also two weak and broad peaks at 3430 and 1630 cm^{-1}, which may be due to the absorbed H_2O in the course of the measurement.

3.1.3. Morphology of the films

Single layer of the $Gd_{1.9}Eu_{0.1}(WO_4)_3$ film has a thickness of about 190 nm, measured by an AUEL-III automatic laser ellipsometer. The morphology of the crystalline $Gd_{1.9}Eu_{0.1}(WO_4)_3$ film sample was inspected using an atomic force microscope (AFM). Fig. 3 shows the AFM images of the transparent $Gd_{1.9}Eu_{0.1}(WO_4)_3$ film annealed at 800°C. It is known from planar image that the film is uniform and crack-free, and mainly consists of closely packed fine particles with an average grain size of 80 nm (planar image in Fig. 3a), and the surface is well crystallized and very smooth with a root mean square (RMS) roughness of 1–2 nm (stereo image in Fig. 3b).

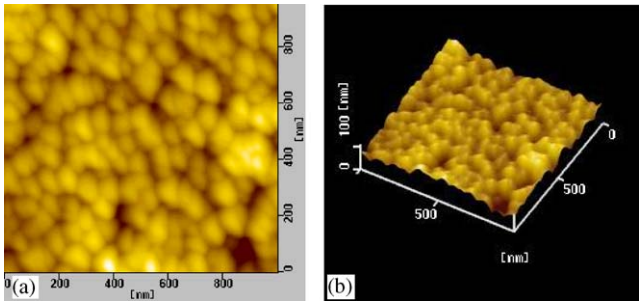

Fig. 3. AFM micrographs of crystalline $Gd_{1.9}Eu_{0.1}(WO_4)_3$ film annealed at 800°C (a) planar image (b) stereo image.

3.2. Photoluminescence properties

3.2.1. Spectral properties of rare earth ions (Eu^{3+} and Dy^{3+})-doped $Gd_2(WO_4)_3$ films

Fig. 4 shows the excitation (a) and emission (b) spectra for $Gd_{1.4}Eu_{0.6}(WO_4)_3$ film annealed at 800°C in the UV/vis spectral range. The excitation spectrum was obtained by monitoring the emission of Eu^{3+} $^5D_0-^7F_2$ transition at 614 nm. It can be seen clearly that the excitation spectrum mainly consists of a broad intense band with a maximum at 263 nm and a shoulder at 252 nm as well as some weak lines in the longer wavelength region. According to Ref. [4], the intensive band at 263 nm should be assigned to the W–O ligand-to-metal charge-transfer states (LMCT) from WO_4 units in the $Gd_2(WO_4)_3$ host lattice, and the shoulder may be due to the Eu–O charge-transfer states. The other weak lines in the longer wavelength region are due to the $f-f$ transitions within Eu^{3+} $4f^6$ electron configuration. The presence of the strong absorption band of WO_4^{2-} groups in the excitation spectrum of Eu^{3+} indicates that there exists an energy transfer from WO_4^{2-} groups to Eu^{3+} ions in $Gd_{1.4}Eu_{0.6}(WO_4)_3$ film. Upon excitation into the WO_4^{2-} absorption band at 263 nm, we can observe the strong emissions corresponding to $^5D_J-^7F_{J'}$ ($J=0$, 1, 2, 3; $J'=0$, 1, 2, 3, 4, not in all cases) transitions of Eu^{3+}. The locations of the emission lines of Eu^{3+} and their assignments are indicated in the Fig. 4b. No intrinsic emission from WO_4^{2-} is observed in the emission spectrum, indicating that an efficient energy transfer from WO_4^{2-} to Eu^{3+} has occurred. The emission spectrum of Eu^{3+} is dominated by the

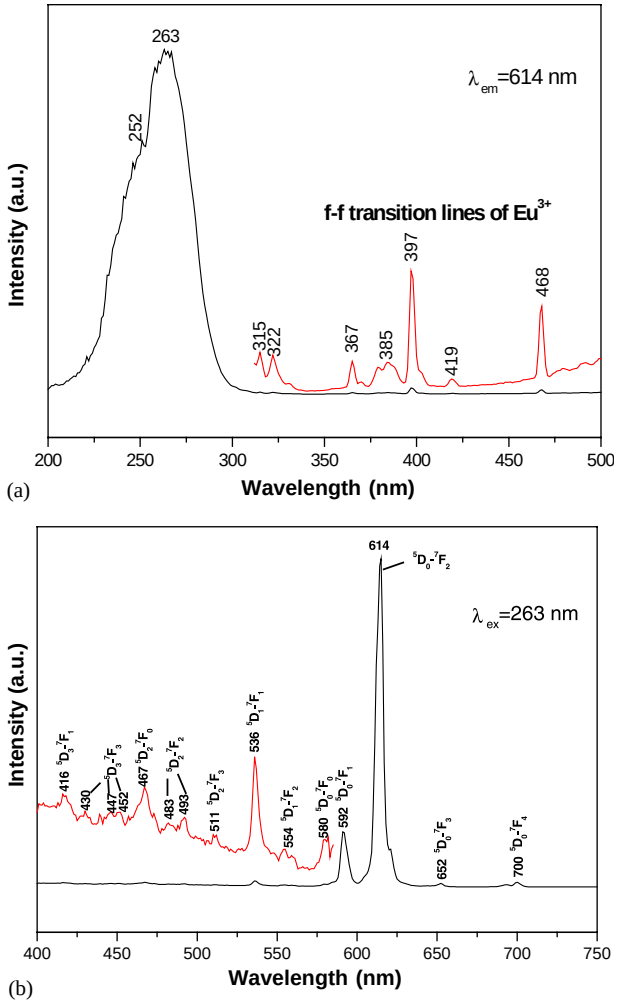

Fig. 4. Excitation (a) and emission (b) spectra of $Gd_{1.9}Eu_{0.1}(WO_4)_3$ film annealed at 800°C.

hypersensitive red emission $^5D_0-^7F_2$ transition of Eu^{3+} at 614 nm (as indicated in Fig. 4b). This indicates that the Eu^{3+} ions are located at sites without inversion center in $Gd_2(WO_4)_3$ films [18], which is in agreement with the crystal structure of $Gd_2(WO_4)_3$. $Gd_2(WO_4)_3$ belongs to space group C_{2h}^6-C2/c with distorted scheelite structure, and very similar to that of $CaWO_4$ [4,19]. The atomic arrangement may be described as a scheelite superlattice with ordered vacancies in the cation positions and considerable distortions of the structure occur around these vacancies [1]. Then it can be concluded that there is no inversion symmetry at the site of the Eu^{3+} ion, and the $^5D_0-^7F_2$ transition dominates in the spectrum. The presence of emission lines from higher excited states of Eu^{3+} ($^5D_1, ^5D_2, ^5D_3$) is attributed to the low vibration energy of WO_4^{2-} groups (850 cm^{-1}, as indicated by Fig. 2). The multi-phonon relaxation by WO_4^{2-} is not able to bridge the gaps between the higher energy levels ($^5D_1, ^5D_2, ^5D_3$) and $^5D_0$ level of Eu^{3+} completely, resulting in the weak emissions from these levels. In silicate and borates where

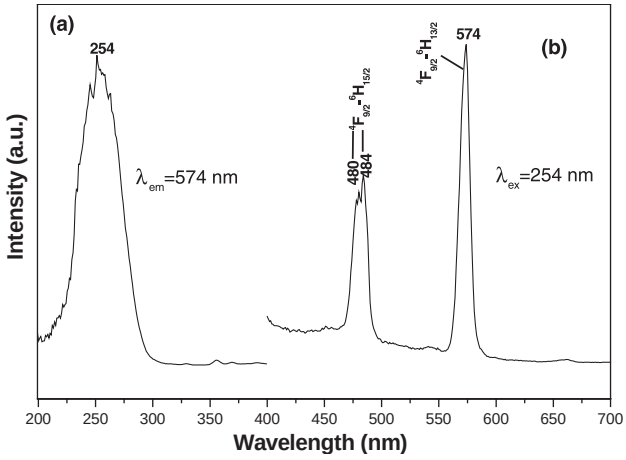

Fig. 5. Excitation (a) and emission (b) spectra of $Gd_{1.88}Dy_{0.12}(WO_4)_3$ film annealed at 800°C.

$\nu_{max} = 1000 \sim 1200\,cm^{-1}$, such emissions cannot be detected [15,18,19].

The same situation holds for the Dy^{3+}-doped $Gd_2(WO_4)_3$ films, as shown in Fig. 5. In the excitation spectra, the WO_4^{2-} excitation band at 254 nm for $Gd_{1.88}Dy_{0.12}(WO_4)_3$ film (Fig. 5a) can be seen clearly, suggesting that the excitations in the films are also mainly via the WO_4^{2-} groups, i.e., an energy transfer from the WO_4^{2-} groups to Dy^{3+} ions also occurs in $Gd_2(WO_4)_3$ films. Upon excitation into the WO_4^{2-} absorption bands at maximum values, the obtained emission spectra contain exclusively the characteristic transition lines of the Dy^{3+} ions, i.e., the lines at 480, 484 nm ($^4F_{9/2}-^6H_{15/2}$) and 574 nm ($^4F_{9/2}-^6H_{13/2}$, dominated) (Fig. 5b).

3.2.1.1. Temperature effects. The lifetimes and PL emission intensity of the rare earth ions (Eu^{3+} and Dy^{3+}) have been studied as a function of annealing temperature in $Gd_2(WO_4)_3$ films. In general, these curves can be fitted into a single exponential function as $I = I_0 \exp(-t/\tau)$ (τ is the $1/e$ lifetime of the rare earth ion). The lifetimes (τ) of excited states for Eu^{3+} ($^5D_0$) and Dy^{3+} ($^4F_{13/2}$) can be determined by the fittings. Table 1 lists the changes of the lifetimes and emission intensity of the rare earth ions (Eu^{3+} and Dy^{3+}) as a function of annealing temperature in $Gd_2(WO_4)_3$ films (the optimum doping concentrations of Eu^{3+} and Dy^{3+} are 30 and 6 at% of Gd^{3+}, respectively). From Table 1 it can be seen that both the lifetimes and PL emission intensity for all the two rare earth ions increase with the increase of annealing temperature from 500°C to 800°C, as observed previously [15–17]. This is because with the increase of annealing temperature the content of impurities in the film such as –OH, NO_3^- and CH_2– and others decreases and the film crystallinity increases (as indicated by XRD results in Fig. 1). The quenching of the luminescence of the rare earth ions by the

Table 1
The effects of the annealing temperatures on the lifetimes (τ) and PL emission intensity (I) of the rare earth ions RE ($RE = Eu^{3+}$ and Dy^{3+}) in $Gd_2(WO_4)_3$ films (the optimum doping concentrations of Eu^{3+} and Dy^{3+} are 30 and 6 at% of Gd^{3+}, respectively)

RE	T (°C)			
	500	600	700	800
Eu^{3+}				
I (a.u.)	15,936	27,350	47,096	66,818
τ (ms)	0.84	0.95	0.96	1.03
Dy^{3+}				
I (a.u.)	33,614	37,917	97,609	100,475
τ (ms)	0.18	0.19	0.19	0.20

vibrations of these impurities decreases, resulting in the increase of their lifetimes and PL emission intensity.

4. Conclusions

Rare earth ions (Eu^{3+} and Dy^{3+}) doped $Gd_2(WO_4)_3$ phosphor films were successfully prepared by the Pechini sol–gel process using the cheap and nontoxic inorganic compounds as main precursors. The rare earth ions Eu^{3+} and Dy^{3+} show their characteristic red ($^5D_0-^7F_2$) and yellow ($^4F_{9/2}-^6H_{13/2}$) emissions in crystalline $Gd_2(WO_4)_3$ phosphor films due to an efficient energy transfer from the WO_4^{2-} to them, respectively. Both the lifetimes and PL intensity of the doped rare earth ions increased with increasing the annealing temperature from 500°C to 800°C, and the optimum doping concentrations of Eu^{3+} and Dy^{3+} are determined to be 30 and 6 at% of Gd^{3+} in $Gd_2(WO_4)_3$ host lattice.

Acknowledgments

This project is financially supported by the foundation of "Bairen Jihua"of Chinese Academy of Sciences, the MOST of China (No. 2003CB314707), and the National Natural Science Foundation of China for Distinguished Young Scholars (50225205).

References

[1] D.H. Templeton, A. Zalkin, Acta Crystallogr. 16 (1963) 762.
[2] K. Nassau, H. Levinstein, G.M. Loiacono, J. Phys. Chem. Solids 26 (1965) 1805.
[3] H.J. Borchardt, J. Chem. Phys. 39 (3) (1963) 504.
[4] C.A. Kodaira, H.F. Brito, M.C.F.C. Felinto, J. Solid State Chem. 171 (1–2) (2003) 401.
[5] J.Y. Choe, D. Ravichandran, S.M. Blomquist, D.C. Morton, K.W. Kirchner, M.H. Ervin, U. Lee, Appl. Phys. Lett. 78 (2001) 3800.
[6] E.M. Rabinovich, J. Shmulovich, V.J. Fratello, N.J. Kopyov, Am. Ceram. Soc. Bull. 6 (1987) 1505.
[7] J. Hao, M. Cocivera, Appl. Phys. Lett. 79 (2001) 740.
[8] J. Hao, J. Gao, M. Cocivera, Appl. Phys. Lett. 82 (2003) 2224.
[9] J. Hao, J. Gao, M. Cocivera, Appl. Phys. Lett. 82 (2003) 2778.
[10] S. Sakka, Struct. Bonding 85 (1996) 1.
[11] D. Ravichandran, R. Roy, A.G. Chakhovskoi, C.E. Hunt, W.B. White, S. Erdei, J. Lumin. 71 (1997) 291.
[12] R.P. Rao, Solid State Commun. 99 (1996) 439.
[13] J. Lin, D.U. Saenger, M. Mennig, K. Baerner, Thin Solid Films 360 (2000) 39.
[14] M.P. Pechini, US Patent 3 330 697, 1967.
[15] M. Yu, J. Lin, Z. Wang, S. Wang, H.J. Zhang, J. Fu, Y.C. Han, Chem. Mater. 14 (2002) 2224.
[16] M. Yu, J. Lin, Y.H. Zhou, S.B. Wang, H.J. Zhang, J. Mater. Chem. 12 (2002) 86.
[17] M. Yu, J. Lin, J. Fu, H.J. Zhang, Y.C. Han, J. Mater. Chem. 13 (2003) 1413.
[18] G. Blasse, B.C. Grabmaier, Luminescent Materials, Springer, Berlin, Heidelberg, 1994.
[19] M.L. Pang, J. Lin, S.B. Wang, M. Yu, Y.H. Zhou, X.M. Han, J. Phys.: Condens. Matter 15 (2003) 5157.